Biomaterials Science

ROYAL SOCIETY OF CHEMISTRY

PAPER

View Article Online
View Journal | View Issue

Cite this: *Biomater. Sci.*, 2022, **10**, 5158

Polyaspartate-derived synthetic antimicrobial polymer enhances the activity of rifampicin against multidrug-resistant *Pseudomonas aeruginosa* infections

Nalini Chaudhary, [a] Bharti Aggarwal, [a] Varsha Saini, [a] Prabhu Srinivas Yavvari, [b] Priyanka Sharma, [c] Aasheesh Srivastava *[b] and Avinash Bajaj *[a]

Received 6th April 2022,
Accepted 24th June 2022

DOI: 10.1039/d2bm00524g

rsc.li/biomaterials-science

Infections caused by multidrug-resistant *Pseudomonas aeruginosa* (*P. aeruginosa*) pose major challenges for treatment due to the acquired, adaptive, and intrinsic resistance developed by the bacteria. Accumulation of mutations, the ability to form biofilms, and the presence of lipopolysaccharides in the outer bacterial membranes are the key mechanisms of drug resistance. Here, we show that a polyaspartate-derived synthetic antimicrobial polymer (SAMP) with a hexyl chain (**TAC6**) is an effective adjuvant for a hydrophobic antibiotic, rifampicin. Our *in vitro* studies demonstrated that the combination of **TAC6** and rifampicin is effective against clinically isolated multidrug-resistant strains of *P. aeruginosa*. Membrane permeabilization studies showed that **TAC6** allows the permeabilization of bacterial membranes, and the accumulation of rifampicin inside the cells, thereby enhancing its activity. The combination of **TAC6** and rifampicin can also degrade the *P. aeruginosa* biofilms, and therefore can mitigate the adaptive resistance developed by bacteria. We further demonstrated that the combination of **TAC6** and rifampicin can clear *P. aeruginosa*-mediated wound infections effectively. Therefore, our study showed polyaspartate-derived SAMP to be an effective antibiotic adjuvant against *P. aeruginosa* infections.

Introduction

Infections caused by multidrug-resistant *Pseudomonas aeruginosa* (*P. aeruginosa*) pose a serious threat as this pathogen can cause bacteremia, severe pneumonia, urinary tract infections, respiratory tract infections and ocular infections.[1,2] *P. aeruginosa* also poses a major threat in skin burns, where it hampers wound healing in patients due to the formation of antibiotic-impenetrable biofilms, thereby leading to chronic infections.[3,4] Biofilm-dwelling *P. aeruginosa* cells tend to have a mutated phenotype with a physiology comparable with that of stationary phase planktonic cells as these cells are deeply embedded under thick biofilms with a lack of nutrients and oxygen.[5] The matrix of the biofilms also provides a physiological barrier to support the persister cells in the biofilms.[6] Therefore, infections caused by *P. aeruginosa* can possess acquired resistance due to the accumulation of mutations or adaptive resistance due to biofilm formation, thereby causing multifaceted challenges for antibiotics.[7] Therefore, there is a need to develop innovative strategies that can mitigate *Pseudomonas aeruginosa* mediated multidrug-resistant infections.[8]

Apart from adaptive and acquired resistance, Gram-negative bacteria also exhibit intrinsic antimicrobial resistance due to the presence of an outer cell membrane that is rich in heavily glycosylated lipids known as lipopolysaccharides (LPSs).[9,10] LPS molecules are crosslinked by divalent cations (Mg^{2+}) through the establishment of ionic bridges among anionic phosphate groups from lipid A. Therefore, LPSs provide a barrier to the majority of hydrophobic antibiotics, and prevent passive diffusion into the bacterial cell.[11,12] As the majority of antibiotics are losing their efficacy over Gram-negative bacteria due to the emergence of resistance, re-sensitisation of Gram-negative bacteria against these antibiotics *via* targeting bacterial cell membranes provides a riveting alternative.[13,14] Antibiotic adjuvants are known to re-sensitize Gram-negative bacteria towards ineffective antibiotics by targeting the efflux pumps, disintegrating bacterial membranes, or enhancing the intracellular accumulation of antibiotics.[15,16] Antibiotic

[a]*Laboratory of Nanotechnology and Chemical Biology, Regional Centre for Biotechnology, NCR Biotech Science Cluster, 3rd Milestone, Faridabad-Gurgaon Expressway, Faridabad-121001, Haryana, India. E-mail: bajaj@rcb.res.in*
[b]*Department of Chemistry, Indian Institute of Science Education and Research, Bhopal By-pass Road, Bhauri, Bhopal-462030, India. E-mail: asrivastava@iiserb.ac.in*
[c]*Department of Microbiology, All India Institute of Medical Sciences, New Delhi-110029, India*

adjuvants do not show any antimicrobial activity but can inhibit the intrinsic and adaptive drug-resistance developed by the bacteria and allow the activity of existing antibiotics.[17–20]

Membrane-permeabilising agents can act as effective antibiotic adjuvants as they can lead to the disruption of bacterial membranes and facilitate the entry of antibiotics into bacterial cells.[21,22] Antimicrobial peptides (AMPs) produced by the host organism's innate immunity tend to perform a similar function due to their amphiphilic nature. AMPs execute electrostatic interactions with bacterial membranes, followed by insertion in them, causing membrane disruptions.[23] However, the clinical utility of these AMPs as antimicrobial agents is restricted due to their instability and toxicity to mammalian cells.[24] Antimicrobial polymers present a suitable alternative to AMPs owing to diversity in their composition and design principles, as they can be derived from a variety of classes including polyamides, polyurethanes, and polycarbonates.[25–27] Cationic polymers tend to target the anionic phosphate groups present in lipid A of the outer bacterial membrane, and compete with the divalent cations involved in cross-bridging. However, many polymer scaffolds are non-biodegradable in nature and can cause long-term toxic effects.[28–30]

Polyaspartic acid is a biodegradable aspartic acid-derived polymer that has been explored for a wide range of biomedical applications including drug and protein delivery, gene therapy, and antimicrobial therapy.[31–34] Recently we have shown that polyaspartate-derived synthetic antimicrobial polymers (SAMPs) are effective antimicrobials against mycobacteria species, and can penetrate the mycobacterial membranes to bind with genomic DNA.[35] Herein, we tested the interactions of these polyaspartate-derived SAMPs with the bacterial membranes of *Pseudomonas aeruginosa*, and tested their efficacy as potential antibiotic adjuvants for rifampicin. We show that **TAC6** acts as an effective adjuvant to rifampicin to alleviate its intrinsic resistance and establish enhanced bactericidal activity. The combination of **TAC6** and rifampicin has also been screened for an auxiliary effect on biofilms and its ability to dissipate wound infections. We demonstrate that the combination of **TAC6** and rifampicin is also effective against multidrug-resistant clinical strains of *P. aeruginosa*.

Results and discussion

Polyaspartate-derived synthetic antimicrobial polymers (SAMPs) are effective permeabilizers

We used five polyaspartate-derived SAMPs (**TAC1**, **TAC2**, **TAC4**, **TAC6**, and **TAC8**) having tetra-alkyl ammonium head groups tethered to the carboxylic acid units through amide bonds. These SAMPs possess varied alkyl chain substitutions like methyl (**TAC1**), ethyl (**TAC2**), butyl (**TAC4**), hexyl (**TAC6**), and octyl (**TAC8**) (Fig. 1A). We first determined the minimum inhibitory concentration (MIC_{99}) of the SAMPs against the wild type strain of *P. aeruginosa* and five multidrug-resistant clinical strains of *P. aeruginosa*. The antimicrobial activities of SAMPs revealed that none of them is an effective antimicrobial against these strains until a concentration of 64–128 mg mL^{-1} is reached (Fig. 1B). To decipher the antibiotic adjuvant ability of these SAMPs against the intrinsic resistance of *P. aeruginosa*, we tested the outer membrane permeabilization abilities of these SAMPs against *P. aeruginosa* using an *N*-phenyl naphthalene (NPN) based fluorescence assay. Quantification of NPN fluorescence on the incubation of NPN-stained *P. aeruginosa* cells with SAMPs (8 μg mL^{-1}) showed a sharp increase in fluorescence in the case of **TAC6** and **TAC8**, whereas there was no significant change in NPN fluorescence on treatment with the other SAMPs (Fig. 1C). These results clearly showed that **TAC6** and **TAC8** can permeabilize the outer bacterial membranes, and can act as effective antibiotic adjuvants.

Rifampicin is a hydrophobic antibiotic that prevents RNA synthesis by the inhibition of DNA-dependent RNA polymerase.[36] Rifampicin is widely used for the treatment of *Mycobacterium* infections in different combination therapeutic regimens owing to its highly hepatotoxic nature.[37] Rifampicin is an effective antibiotic against Gram-positive cocci as well but is less effective against Gram-negative bacteria.[38] Therefore, there is a need to develop strategies to enhance the antimicrobial activity of rifampicin against Gram-negative bacteria, especially *P. aeruginosa*. The hemolytic activities showed that **TAC8** is highly hemolytic with an HC_{10} of 128 μg mL^{-1}, whereas the other polymers are non-hemolytic even at 1000 μg mL^{-1} (Fig. 1B).[35] Similarly, the cytotoxicity results against HEK-293 cells witnessed that the **TAC8** polymer is highly toxic (Fig. 1B).[35] Therefore, we pursued further studies with **TAC6** to test its antibiotic adjuvant potential.

TAC6 acts as a potential adjuvant for rifampicin

To test the efficacy of **TAC6** as an antibiotic adjuvant, we performed a chequerboard assay, and screened combinations of different concentrations of **TAC6** and rifampicin for their synergistic antimicrobial activity against *P. aeruginosa* (MTCC1688). The synergy was assessed using the fractional inhibitory concentration (FIC) index where a FIC index value <0.5 indicates synergy. We observed that **TAC6** and rifampicin alone exhibited MIC_{99} values of 128 and 8 μg mL^{-1} respectively against *P. aeruginosa* (Table 1). The screening of different combinations of **TAC6** and rifampicin showed that a combination of **TAC6** (8 μg mL^{-1}) and rifampicin (1 μg mL^{-1}) was sufficient to clear the microbial culture (Fig. 2A). To elucidate the synergy of **TAC6** and rifampicin across different multidrug-resistant strains, we screened the combination of **TAC6** and rifampicin against five different multidrug-resistant clinical strains of *P. aeruginosa*. We observed that **TAC6** (8 μg mL^{-1}) was able to enhance the antimicrobial activity of rifampicin against other multidrug-resistant clinical strains as well (Fig. 2B–F). The synergy curves show a decrease in the MIC_{99} of rifampicin on increasing the concentration of **TAC6** against all *P. aeruginosa* strains (Fig. 3). We observed that 8 μg mL^{-1} of **TAC6** was sufficient to decrease the MIC_{99} of rifampicin from 8 μg mL^{-1} to 1–2 μg mL^{-1} (Fig. 3). A comparison of the anti-

A

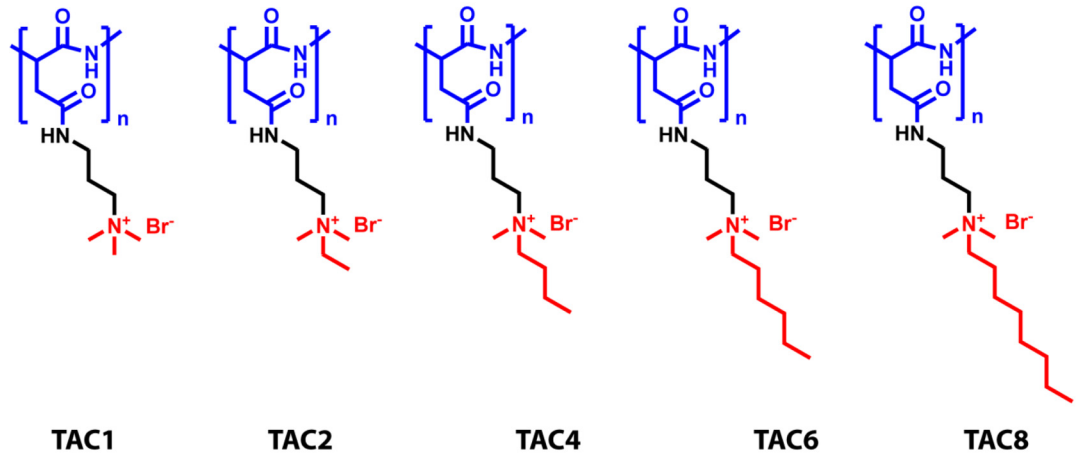

B

	MIC_{99} (μg/mL)[a]	IC_{50} (μg/mL)[b]	HC_{10} (μg/mL)[c]
TAC1	>128	>512	>1000
TAC2	>128	>512	>1000
TAC4	>128	256	>1000
TAC6	128	128	>1000
TAC8	64	50	128

a: Minimum inhibitory concentration against *P. aeruginosa*.
b: Cytotoxicity against HEK-293 cells.[35]
c: Hemolytic activity against RBCs.[35]

C

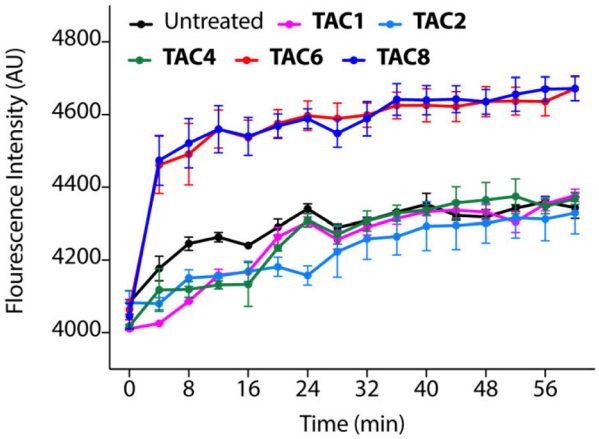

Fig. 1 (A) Molecular structures of polyaspartic acid-derived SAMPs with varied hydrophobicity. (B) Minimum inhibitory concentrations (MIC_{99}), cytotoxicity, and hemolytic activity of polyaspartic acid-derived SAMPs against *P. aeruginosa*, HEK-293 cells, and human RBCs respectively. (C) Change in NPN fluorescence on incubation of NPN-stained *P. aeruginosa* cells with polyaspartic acid-derived SAMPs. Data in (B) are the means of three independent replicates, and data in (C) are presented as the means ± SDs of three independent replicates.

Table 1 Antimicrobial activities (MIC_{99}), fractional inhibitory concentration (FIC) index, and the potentiation of RIF in the presence of **TAC6** against different *P. aeruginosa* strains

	MIC_{99} (μg mL^{-1})					
	When used alone		When used in combination			
	TAC6	RIF	**TAC6**	RIF	FIC index	Potentiation
P. aeruginosa	128	8	8	1	0.1875	8
P. aeruginosa (9/7P)	128	8	8	2	0.3125	4
P. aeruginosa (1/318)	128	8	4	1	0.15625	8
P. aeruginosa (2/783)	128	8	4	1	0.1875	8
P. aeruginosa (7/233)	128	8	4	2	0.28125	4
P. aeruginosa (6/264)	128	8	32	2	0.5	4

microbial activity of the combination of **TAC6** and rifampicin against different strains witnessed that **TAC6** is an effective adjuvant against five of the six strains with FIC values of <0.5, and showed an additive effect in only one *P. aeruginosa (6/264)* strain (Table 1). We also observed 4–8 fold increase in the potentiation of rifampicin on using it in combination with

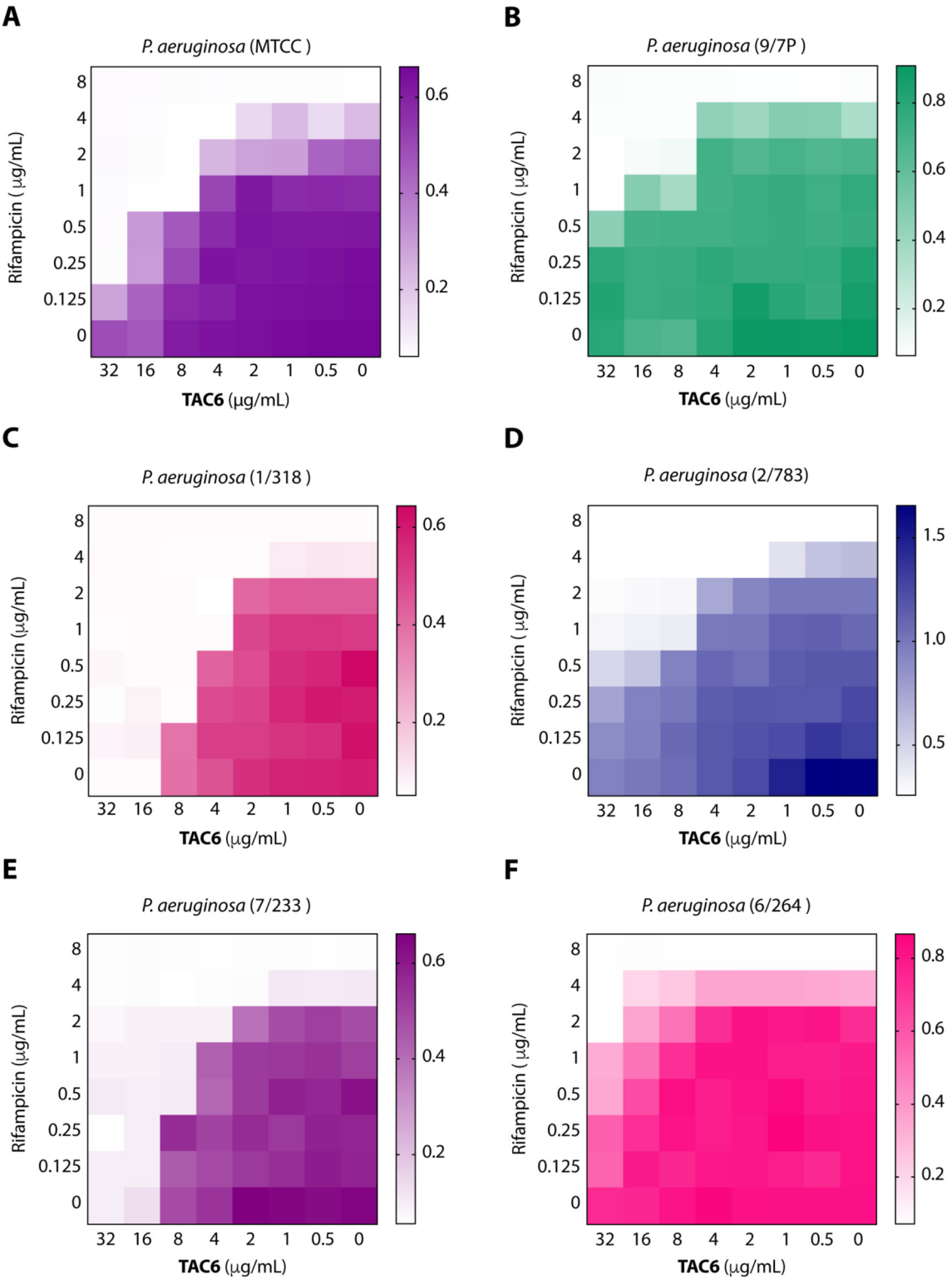

Fig. 2 Heat maps (A–F) showing the effect of **TAC6** on antimicrobial activity of rifampicin against different *P. aeruginosa* strains.

TAC6 (Table 1). Therefore these results clearly demonstrated that **TAC6** is a potential antibiotic adjuvant that enhances the activity of rifampicin against multidrug-resistant clinical *P. aeruginosa* strains.

TAC6 permeabilizes the bacterial membrane for rifampicin

To evaluate the efficacy of a combination of **TAC6** and rifampicin against bacterial growth, we performed time-dependent

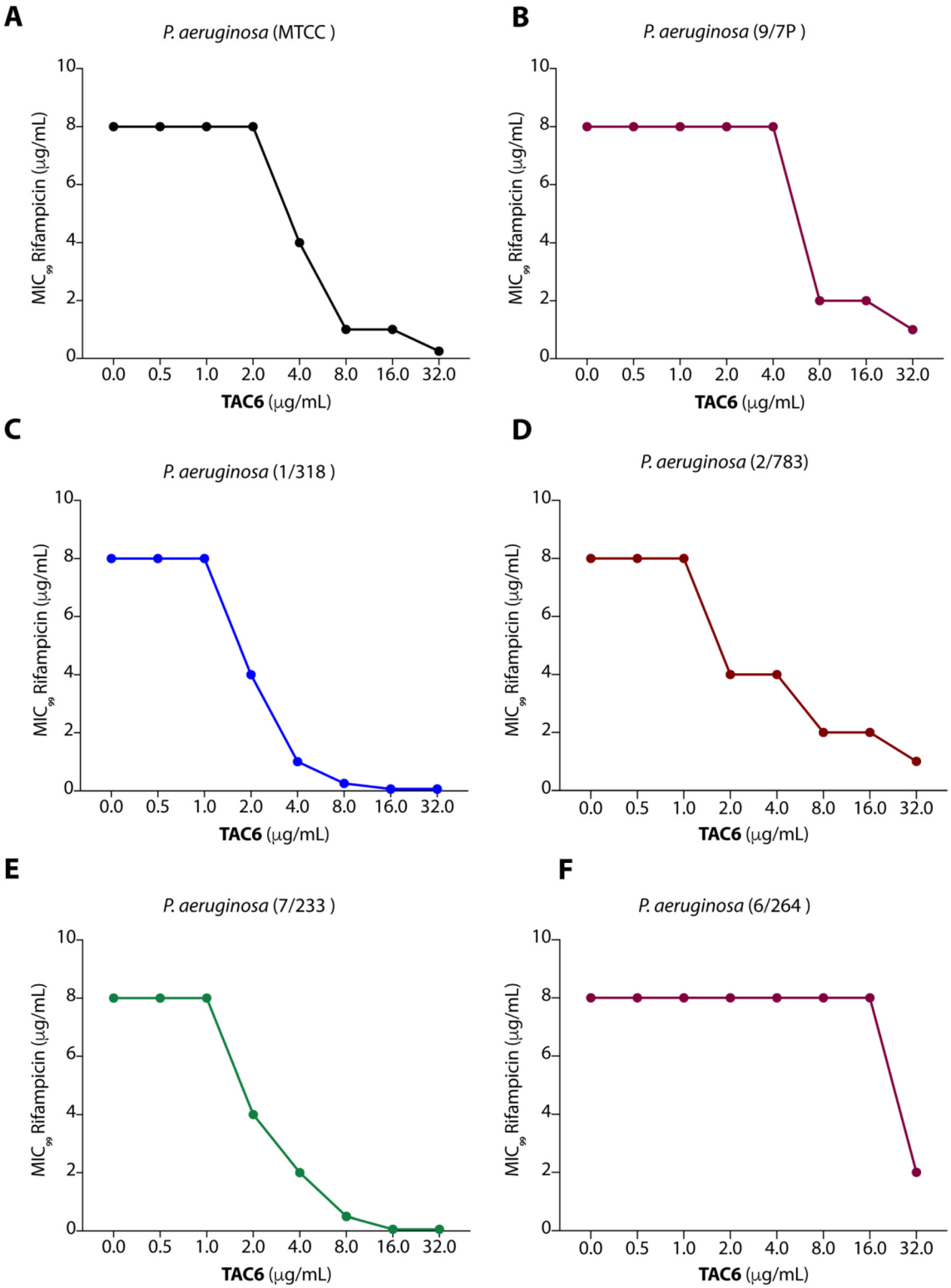

Fig. 3 Synergy curves (A–F) showing the effect of **TAC6** on the antimicrobial activity of rifampicin against different *P. aeruginosa* strains. Data are presented as the means of three independent replicates.

growth and killing assays. The growth kinetics of untreated bacterial cells evaluated by absorbance at 600 nm for 12 h showed a typical sigmoidal curve, and treatment with a combination of **TAC6** (8 μg mL^{-1}) and rifampicin (1 μg mL^{-1}) witnessed no bacterial growth (Fig. 4A). In contrast, treatment with only **TAC6** (8 μg mL^{-1}) or only rifampicin (1 μg mL^{-1}) did

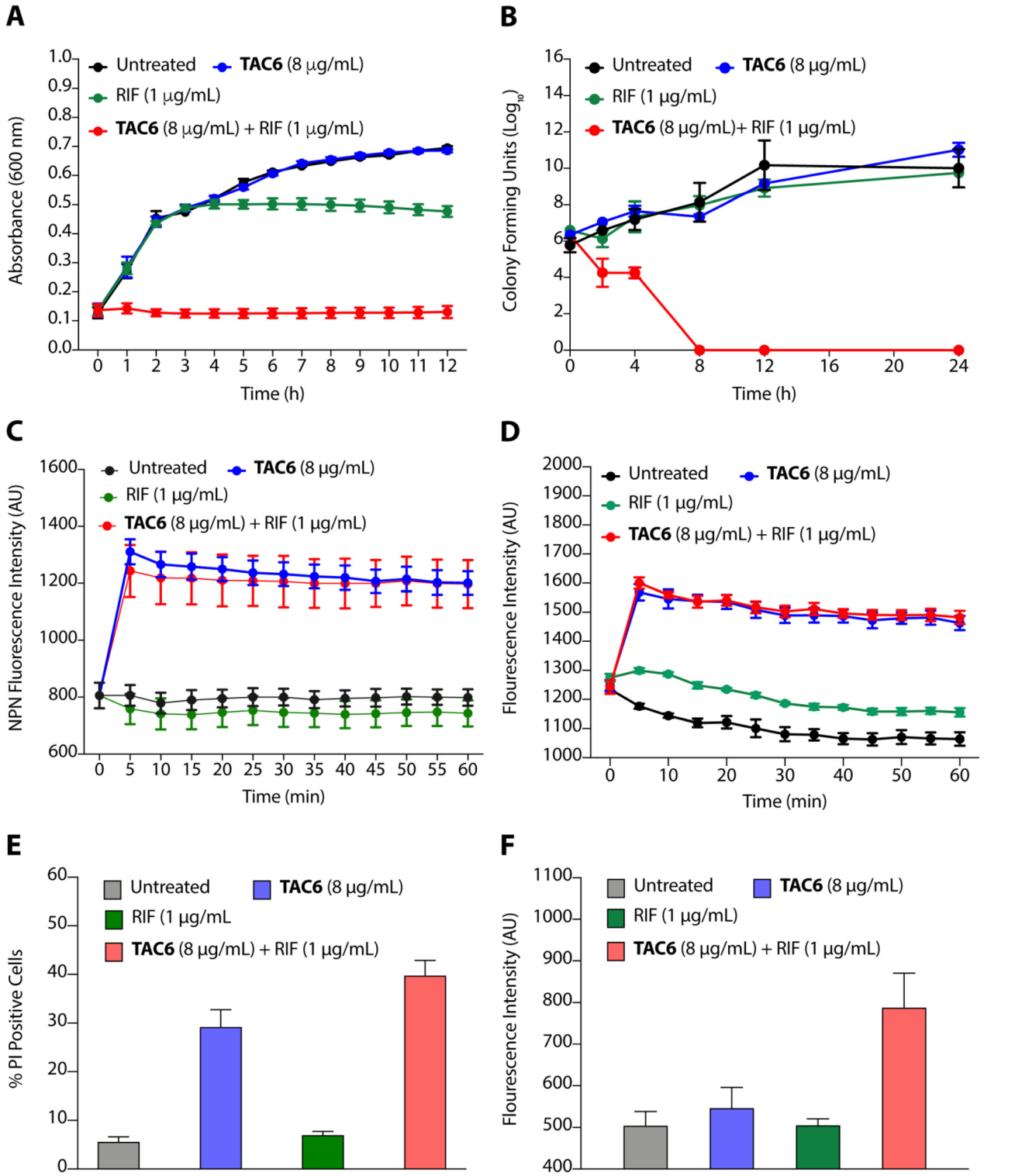

Fig. 4 (A) Growth kinetic assay of *P. aeruginosa* in the presence of **TAC6**, rifampicin, and a combination of **TAC6** and rifampicin. (B) Time–kill kinetic assay upon treatment of *P. aeruginosa* with **TAC6**, rifampicin, and a combination of **TAC6** and rifampicin. (C and D) Change in NPN (C) and DiSC2(5) (D) fluorescence upon treatment of NPN- and DiSC2(5)-stained *P. aeruginosa* with **TAC6**, rifampicin, and a combination of **TAC6** and rifampicin. (E) Percentage of PI-positive *P. aeruginosa* cells upon treatment of *P. aeruginosa* with **TAC6**, rifampicin, a and combination of **TAC6** and rifampicin. RIF in the figure represents rifampicin. (F) Quantification of DCF fluorescence indicating the ROS levels upon treatment of *P. aeruginosa* with **TAC6**, rifampicin, and a combination of **TAC6** and rifampicin. Data in above figures are presented as means ± SDs of three independent replicates.

not show any significant decrease in bacterial growth (Fig. 4A). These findings were further substantiated by a 24 h time–kill assay, where bacterial cell death upon different treatments was evaluated by colony forming units at each time point. The results signified a complete abolition of the bacterial population within 8 h of treatment with a combination of **TAC6** (8 μg mL^{-1}) and rifampicin (1 μg mL^{-1}) (Fig. 4B). Next, we used dye-based assays to clarify the hypothesis of outer membrane disruptions as a possible route for the potentiation of rifampicin activity. An NPN dye assay was performed for the scrutiny of membrane permeabilization upon treatment with a combination of **TAC6** (8 μg mL^{-1}) and rifampicin (1 μg mL^{-1}). Significant increases in NPN fluorescence upon treatment with the combination therapy confirmed the successful permeabilization facilitating the entry of rifampicin into bacterial cells, thereby leading to bactericidal action (Fig. 4C).[39] The permeabilization of the inner membrane was investigated using a membrane potential-sensitive dye, $DiSC_2(5)$ (3,3-diethylthiacarbocyanine iodide), that accumulates within the inner membrane and gets quenched.[40] Treatment of **TAC6** alone or in combination with rifampicin caused a sharp increase in fluorescence intensity (Fig. 4D). We also demonstrated the effect of combination therapy on membrane integrity using the propidium iodide (PI) uptake assay, and observed 40% more PI-positive cells using a combination of **TAC6** (8 μg mL^{-1}) and rifampicin (1 μg mL^{-1}) compared with treatment with **TAC6** alone (Fig. 4E). We validated the bactericidal action using a combination of **TAC6** (8 μg mL^{-1}) and rifampicin (1 μg mL^{-1}) by quantifying the reactive oxidative species (ROS) using DCFH-DA (2′,7′-dichlorofluorescin diacetate). The ROS generated after cellular damage oxidise DCFH-DA to the fluorescent 2′,7′-dichlorofluorescein (DCF).[41] We observed a ∼2-fold increase in fluorescence intensity upon treatment with a combination of **TAC6** and RIF, confirming the bactericidal effect (Fig. 4F). Therefore, these results clearly demonstrate the membrane-permeabilizing ability of **TAC6** that enhances the uptake of rifampicin by bacteria, causing bactericidal action.

Lipopolysaccharides of outer bacterial membranes are a potential target for TAC6

The outer leaflet of the outer membrane of Gram-negative bacteria consists of a lipopolysaccharide layer (LPSs) comprising lipid A with cross-linkages of divalent cations like Mg^{2+} and Ca^{2+}.[42] As LPSs are the main cause of intrinsic resistance developed by Gram-negative bacteria, we deciphered the effect of LPSs (50 μg mL^{-1}) on the antimicrobial activity of a combination of **TAC6** and rifampicin against *P. aeruginosa*. We observed that the incubation of LPSs inhibits the synergistic antimicrobial effect of a combination of **TAC6** and rifampicin as bacteria need 16 μg mL^{-1} (an 8-fold increase) of rifampicin in combination with 2 μg mL^{-1} of **TAC6** in the presence of LPSs (Fig. 5A). Quantification of PI-positive cells treated with a combination of **TAC6** and rifampicin further witnessed a >8-fold decrease in the percentage of PI-positive cells in the presence of LPS (Fig. 5B). Therefore, these results suggest that LPSs interact with **TAC6** and inhibit the membrane permeabilization.

We also tested for the effect of monovalent (Na^+) and divalent (Mg^{2+}) cations on the synergistic activity of **TAC6** and rifampicin against *P. aeruginosa*. Monovalent (Na^+) cations induced no significant change in the activity of a combination of **TAC6** and rifampicin, whereas divalent (Mg^{2+}) cations inhibited the synergy as we observed an 8-fold increase in the MIC_{99} of rifampicin in the presence of divalent (Mg^{2+}) cations (Fig. 5C). The PI uptake assay further demonstrated that the presence of divalent (Mg^{2+}) cations inhibits the **TAC6**-mediated uptake of PI by *P. aeruginosa* cells (Fig. 5D). Therefore, these results clearly confirm that **TAC6** interacts with the LPSs of Gram-negative bacteria, displaces the Mg^{2+} ions, and permeabilizes the bacterial membranes. This **TAC6**-mediated permeabilization of bacteria allows the influx of rifampicin, and is responsible for the synergistic therapeutic effect of the combination of **TAC6** and rifampicin.

The combination of TAC6 and rifampicin can clear bacterial biofilms

Bacterial biofilms are assemblies of bacterial cells within a polysaccharide matrix, and pose a serious challenge for treatment due to the decreased penetration of antibiotics into the matrix.[43] A significant effect of biofilm formation is experienced in clinical settings where medical devices and other surfaces provide a great opportunity for biofilm formation, presenting a cause of nosocomial infections.[43] Therefore, we quantified the biofilm eradication on using the combination of **TAC6** with rifampicin. We assessed the time-dependent eradication of *P. aeruginosa* biofilms upon treatment of biofilms with only **TAC6**, only rifampicin, and using a combination of **TAC6** and rifampicin. The quantification of colony forming units at various time points post treatment witnessed a time-dependent decrease (Fig. 6A). We observed a ∼3-log reduction after 8 and 12 h of treatment with a combination of **TAC6** and rifampicin as compared with untreated biofilms (Fig. 6A). The quantification of CFUs after 12 h of treatment showed ∼1-log decrease on treatment with **TAC6** or rifampicin alone as compared with untreated biofilms, and no effect as compared with the initial biofilm load (Fig. 6A). We observed that a combination of **TAC6** and rifampicin caused a >4-log decrease in CFUs as compared with untreated biofilms after 12 h of treatment (Fig. 6A and B).

The biofilm degradation properties of combination of **TAC6** and rifampicin were further validated by staining of the untreated and treated *P. aeruginosa* biofilms upon SYTO9/PI staining.[44] Untreated biofilms showed a thick mass of biofilms having live SYTO9-stained cells (Fig. 6C). Fluorescence micrographs of treated biofilms witnessed that a combination of **TAC6** and rifampicin can degrade the pre-formed *P. aeruginosa* biofilms successfully (Fig. 6C). Therefore, these results demonstrate that the combination therapy of **TAC6** and rifampicin is an effective strategy for clearing biofilms.

The combination of TAC6 and rifampicin can clear wound infections

P. aeruginosa is one of the key pathogens responsible for wound infections along with *S. aureus*.[45,46] Therefore, we

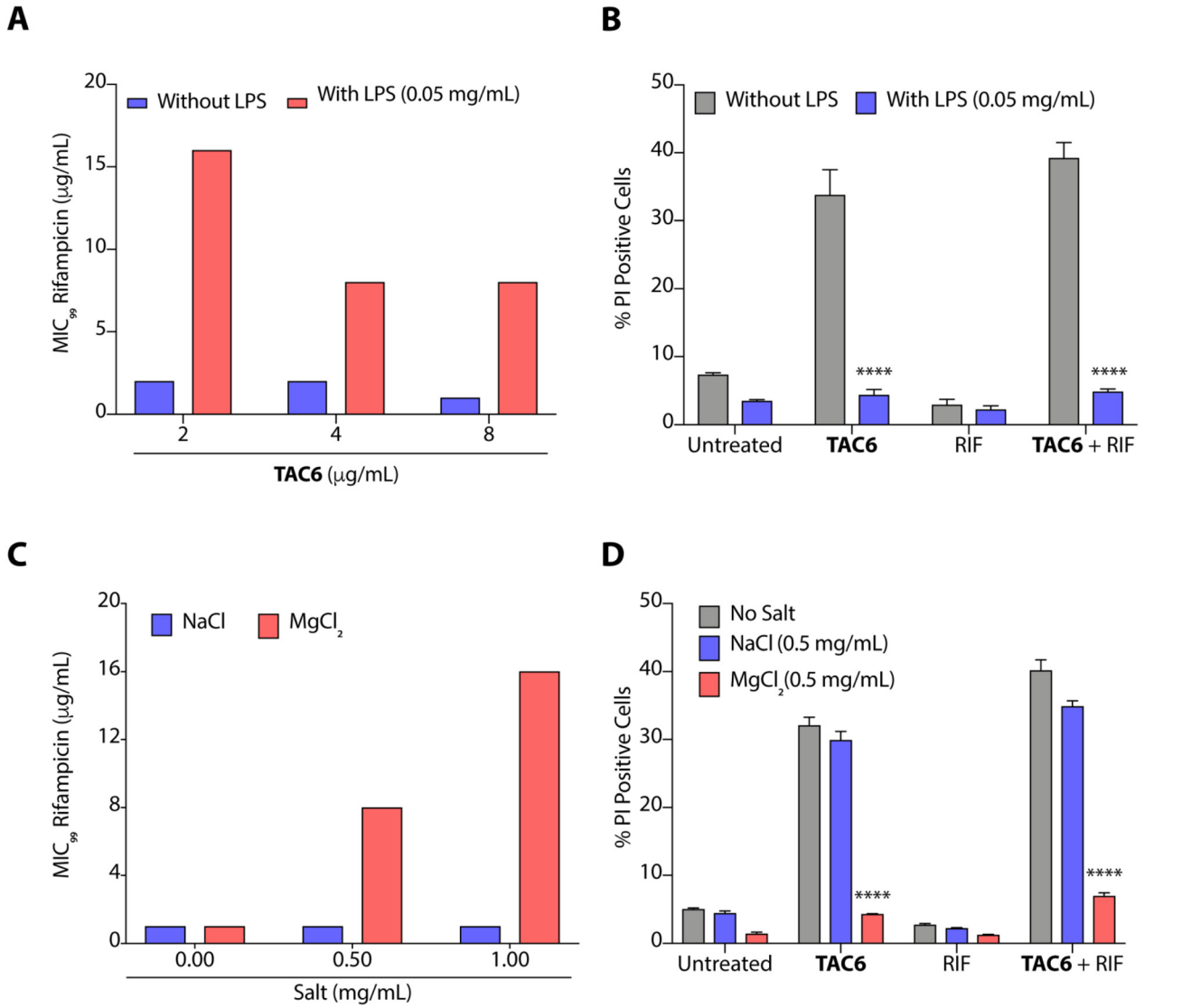

Fig. 5 (A) Change in MIC_{99} of rifampicin in the absence and presence of LPSs upon using it in combination with **TAC6** against *P. aeruginosa*. (B) Change in % PI-positive *P. aeruginosa* cells upon treatment with **TAC6** (8 μg mL^{-1}), rifampicin (1 μg mL^{-1}) or a combination of **TAC6** (8 μg mL^{-1}) and rifampicin (1 μg mL^{-1}) in the absence and presence of LPSs. (C) Change in the MIC_{99} of rifampicin in the absence and presence of Na^+ and Mg^{2+} ions upon using it in combination with **TAC6** against *P. aeruginosa*. (D) Change in % PI-positive *P. aeruginosa* cells upon treatment with **TAC6** (8 μg mL^{-1}), rifampicin (1 μg mL^{-1}) or a combination of **TAC6** (8 μg mL^{-1}) and rifampicin (1 μg mL^{-1}) in the absence and presence of Na^+ and Mg^{2+} ions. Data in (A) and (C) are the means of three independent replicates, and data in (B) and (D) are presented as the means ± SD of three independent replicates.

tested the effect of the combination of **TAC6** and rifampicin in a wound infection model using *P. aeruginosa* in BALB/c mice. Circular skin wounds on BALB/c male mice were infected with *P. aeruginosa* for 24 h, and infected mice were randomized into four groups. Among the different groups, group 1 mice were left untreated, and a second group of mice were treated with **TAC6** (10 mg kg^{-1}) three times a day for three days. The mice in the third group were treated with rifampicin (5 mg kg^{-1}) for three days, and group 4 mice were treated with a combination of **TAC6** (10 mg kg^{-1}) and rifampicin (5 mg kg^{-1}) for three days (Fig. 7A). On the fourth day, the wound sites were homogenised with a post-surgical incision and scrutinised for colony forming units by plating on LB agar plates. Quantification of CFUs showed a >2-log fold reduction on treatment with the combination of **TAC6** and rifampicin as compared with the control group and rifampicin treatment (Fig. 7B). Of note, the combination treatment of rifampicin (5 mg kg^{-1}) and **TAC6** (10 mg kg^{-1}) showed potent synergistic activity, while rifampicin alone, which is able to clear the microbes at 8 μg mL^{-1} (1× MIC) in an *in vitro* setting, fails in animal studies. This could be due to the tolerance of *P. aeruginosa* to rifampicin at this concentration. Moreover, **TAC6** (10 mg kg^{-1}) shows minor reductions in infection, suggesting that **TAC6** is sensitizing the bacterial cells. These results clearly validate the efficacy of the combination treatment against *P. aeruginosa* in wound infections.

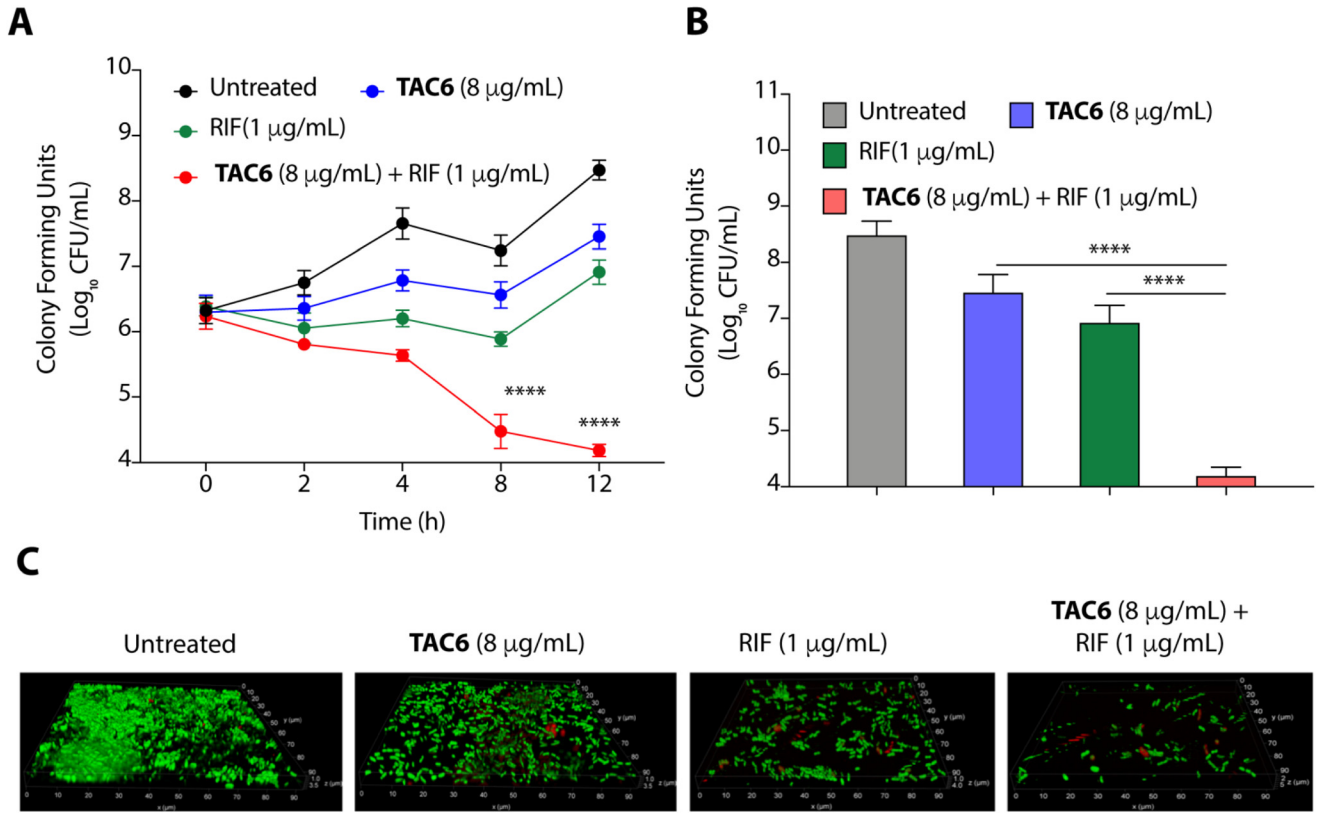

Fig. 6 (A) Time-dependent change in CFUs of preformed *P. aeruginosa* biofilms on treatment with **TAC6**, rifampicin, and a combination of **TAC6** and rifampicin witnesses the synergistic bactericidal effect on biofilms. (B) Change in CFUs after 12 h of treatment of *P. aeruginosa* biofilms with **TAC6**, rifampicin, and a combination of **TAC6** and rifampicin confirms the anti-biofilm effect of combination therapy. (C) Fluorescence micrographs of SYTO9/PI-stained untreated and treated *P. aeruginosa* biofilms demonstrate the bactericidal effect. Data in (A) and (B) are presented as means ± SD of three independent replicates.

Conclusions

Rifampicin hampers the DNA-dependent RNA polymerase activity of most bacterial genera including mycobacteria and Gram-positive bacteria. The efficacy of rifampicin is restricted against Gram-negative bacteria because of the impermeable LPS outer membrane. To overcome this coldness of rifampicin against Gram-negative bacteria and sensitize these bacterial cells towards rifampicin, various studies have used adjuvant molecules. In one study, the authors screened a library of short linear antibacterial peptides (SLAPs) in combination with different antibiotics like rifampicin, tetracycline, vancomycin, cefepime, and ofloxacin using a chequerboard assay, and disclosed that MDR *E. coli* B2, which has 25 antibiotic-resistant genes, was effectively killed by a synergistic combination of SLAP-S25 and antibiotics at sub-MIC.[21] Our study also showed that rifampicin with **TAC6** molecule efficiently inhibits multidrug-resistant *P. aeruginosa* cells. The membrane disrupting effects of the adjuvant **TAC6** are not limited to the outer membrane but **TAC6** also depolarizes the inner bacterial membrane without causing any cell death. An anti-protozoal drug, pentamidine, also perturbs the Gram-negative outer membrane through its interactions with LPSs, and allows the entry of hydrophobic drugs like rifampicin and colistin.[22] As addition of exogenous LPSs and Mg^{2+} ions abolishes the **TAC6**-dependent potentiation of rifampicin, these results suggest that the **TAC6**-like pentamidine targets LPSs and competes with Mg^{2+} ions to disrupt the tight joint between the two side-by-side lipid chains of LPSs, and increases the permeability of outer membrane.[47] In another study, a lysine-based small molecule has been shown to cause a synergistic antimicrobial effect with rifampicin and tetracycline in mitigating Gram-negative bacterial cells and fully grown biofilms, and to remain active under *in vivo* conditions.[13] Similarly, our results confirmed that a combination of **TAC6** and rifampicin can cause the degradation of fully grown biofilms and clear wound infections. Therefore, this study reveals the antibiotic adjuvant effect of polyaspartate-derived polymers that can enhance the activity of rifampicin against multidrug-resistant Gram-negative *P. aeruginosa* bacteria (Fig. 8), and will help in the design of future effective antibiotic adjuvants.

Experimental section

Materials

The tryptone soya broth (TSB) (Cat # M011), LB broth (Cat # M1245), rifampicin (Cat # CMS1889) and bacteriological agar

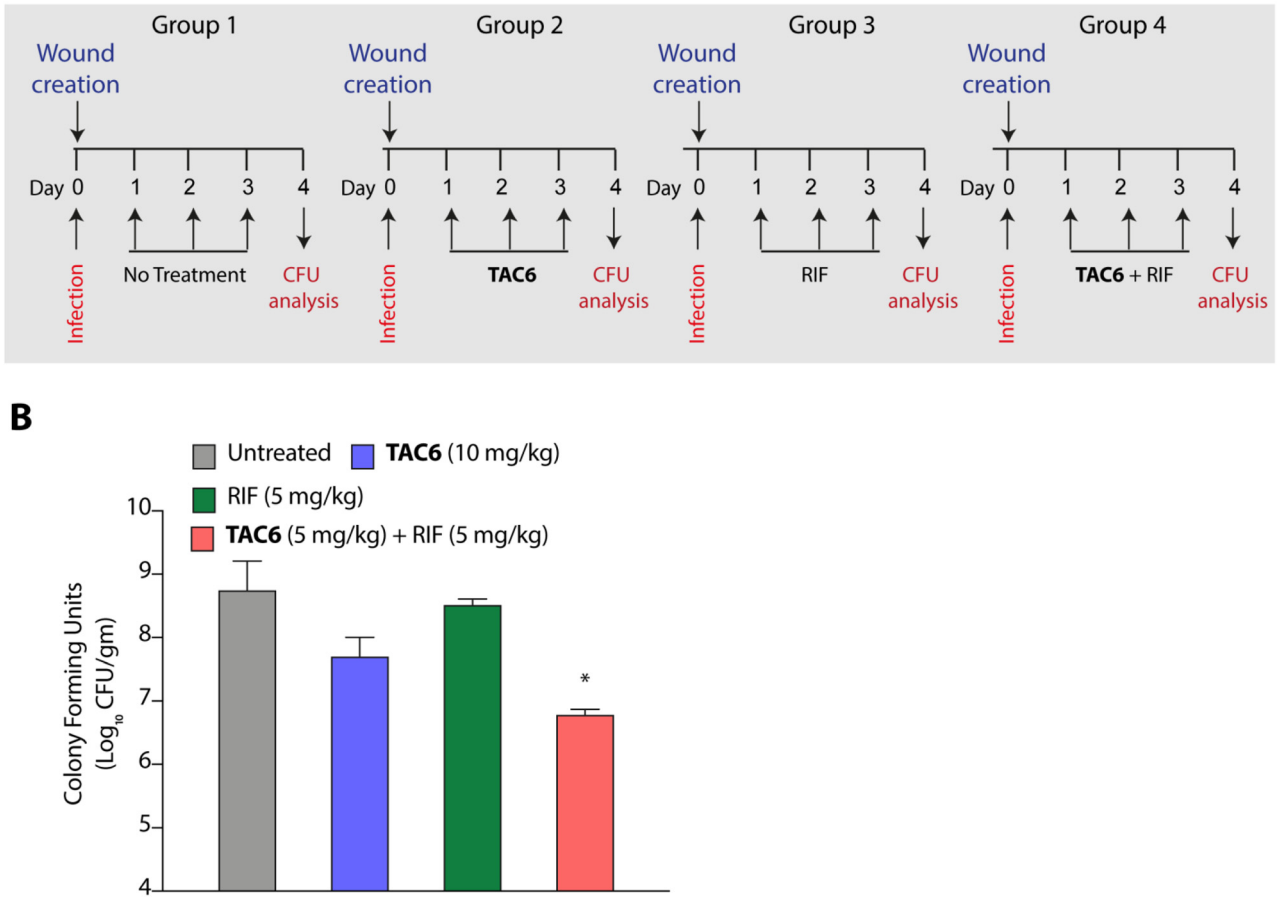

Fig. 7 (A) Schematic showing the experimental plan to test the efficacy of a combination of **TAC6** and rifampicin against *P. aeruginosa* wound infections. (B) Quantification of bacterial burden on different treatments. Data in (B) are presented as means ± SD (n = 4 animals per group).

(Cat # GRM026) used for culturing different strains were purchased from HiMedia, India. Ciprofloxacin (Cat # 17850), propidium iodide (Cat # P1470), lipopolysaccharides from *Escherichia coli* O111:B4 (Cat # 1_4130), 3,3-diethylthiadicarbocyanine iodide (Cat # 17375), magnesium chloride (Cat # M8266), sodium chloride (Cat # 106404), and 2′,7′-dichlorofluorescein diacetate (Cat # 35845) were procured from Sigma-Aldrich, USA. The LIVE/DEAD® BacLight™ bacterial viability and counting kit was from Invitrogen, USA, and *Pseudomonas aeruginosa* (MTCC1688) were purchased from the MTCC (Chandigarh, India).

Polymer synthesis and characterization. All the polymers (**TAC1–TAC8**) were synthesized and characterized as published previously.[35]

Antibacterial activity. Polymers were screened against various bacterial strains to obtain the minimum inhibitory concentrations (MIC_{99}) as per the protocol guidelines provided by the CLSI (Clinical Laboratory Standards Institute).[48] *Pseudomonas aeruginosa* cells were cultured overnight in Luria Bertani broth (LB) media, and cultured cells were centrifuged at 5000 rpm for 5 min followed by resuspension in fresh media, adjusting the concentration to 10^6 cells per mL. Polymeric solutions (100 μL in volume) were serially diluted to obtain concentrations ranging from 128 to 0.5 μg mL^{-1} in a 96-well microtiter plate. Subsequently, 100 μL of bacterial suspension was inoculated into the wells. The plates were incubated for a period of 14–16 h at 37 °C, and their optical density was evaluated through measurement of the absorbance values at a wavelength of 600 nm using a Spectramax M5 multimode microplate reader (Molecular Devices, Sunnyvale, CA, USA). Polymyxin B, a polypeptide antibiotic with specific activity against Gram-negative bacteria was kept as a positive control.

Chequerboard assay. Log phase cultures of different strains were grown in LB broth. A bacterial suspension with about 10^6 cells per mL was treated with various concentrations of rifampicin and **TAC6**. Microdilutions for both **TAC6** and rifampicin were made in multichannel dams by serial dilution. **TAC6** was diluted along the abscissa, and rifampicin was diluted along the ordinate in a 96-well microtiter plate. MIC_{99} was obtained by measuring the absorption at 600 nm after 18 h of treatment at 37 °C using a Spectramax M5 multimode microplate reader (Molecular Devices, Sunnyvale, CA, USA). The FICI

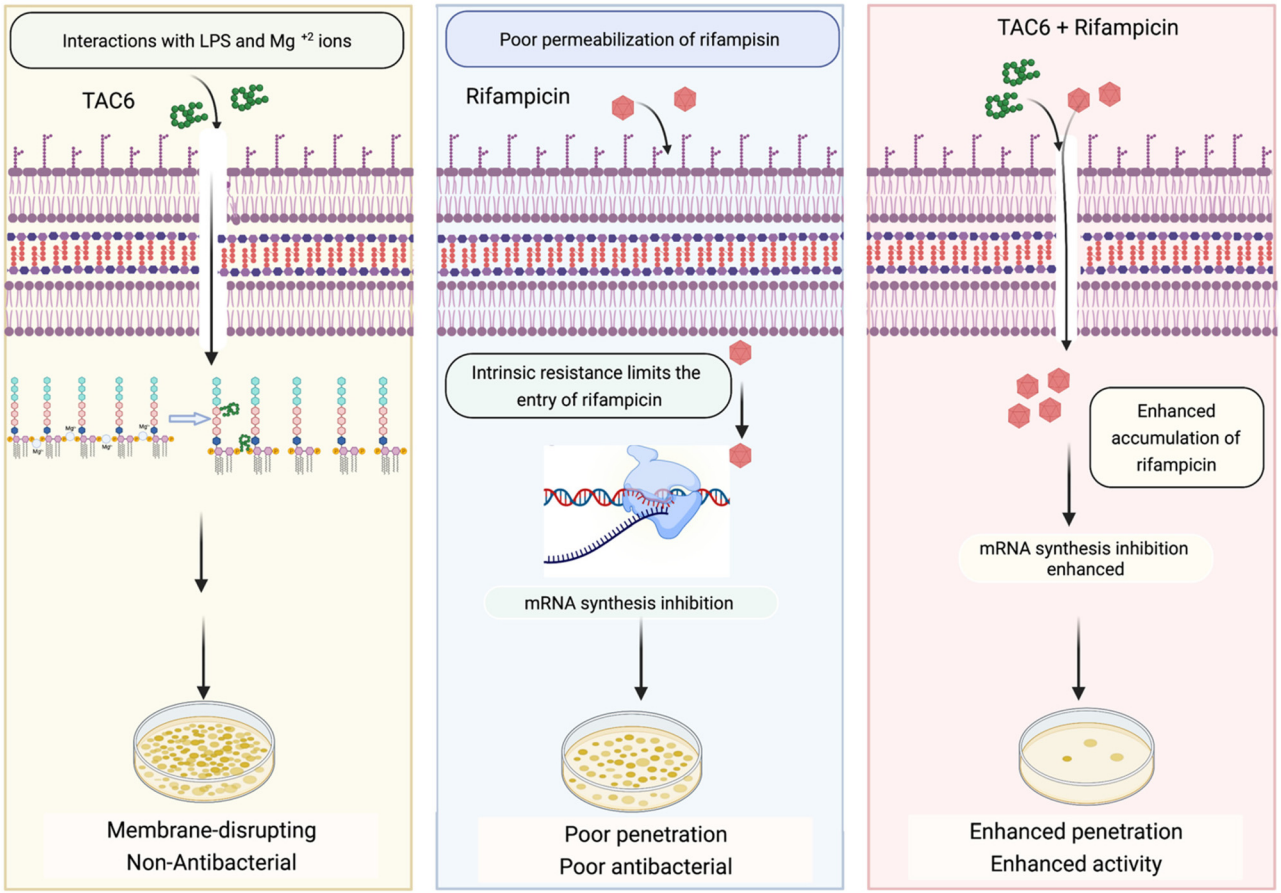

Fig. 8 Schematic showing the ability of **TAC6** to enhance the therapeutic efficacy of rifampicin and enhance its permeation through bacterial membranes.

(FIC Index) was calculated using the following formula: FIC Index = ($MIC_{rifampicin\ in\ combination}/MIC_{rifampicin\ alone}$) + ($MIC_{\mathbf{TAC6}\ in\ combination}/MIC_{\mathbf{TAC6}\ alone}$).[49]

To check the effect of LPSs on synergy, the **TAC6** solution was incubated with LPSs (50 μg mL^{-1}) for 30 min before dilution in a 96-well plate along the abscissa. Similarly, to check the effect of monovalent and divalent cations, bacterial suspension cells were incubated with 0.5 mg mL^{-1} of salts before dilution along the ordinate.

Growth inhibition kinetics. *P. aeruginosa* were cultured up to log phase in LB media, followed by centrifugation at 5000 rpm for 5 min, and cells were then resuspended in fresh media to 10^6 cells per mL. Bacterial cells were treated with **TAC6** at 8 μg mL^{-1} and rifampicin at 1 μg mL^{-1}, and with a combination of **TAC6** (8 μg mL^{-1}) and rifampicin (1 μg mL^{-1}). Cells were subjected to different treatments in a 96-well microtiter plate, and the growth kinetics was measured by obtaining the absorbance values at 600 nm at regular intervals using a Spectramax M5 multimode microplate reader (Molecular Devices, Sunnyvale, CA, USA).

Bactericidal time–kill kinetic study. Bacterial cells were cultured to log phase in LB media, and centrifuged at 5000 rpm for 10 min. Cells were resuspended in fresh media to form a bacterial suspension of 10^6 cells per mL. The bacterial suspension was treated with **TAC6** at 8 μg mL^{-1} and rifampicin at 1μg mL^{-1}, and with a combination of **TAC6** (8 μg mL^{-1}) and rifampicin (1 μg mL^{-1}) for various time points (0, 2, 4, 8, 12, and 24 h) at 37 °C. Untreated and treated bacterial suspension cells were serially diluted after each time point and plated on LB-Agar plates. These plates were kept for incubation at 37 °C for 16–18 h. The colonies on each plate were counted, and the bacterial load was expressed in terms of $\log_{10}$ CFU per mL as a function of time.

Outer membrane permeabilizing assay. To quantify the ability of polymers to disrupt the outer membrane, a dye-based assay was conducted. Bacterial cells from log phase culture were washed and diluted in 1× PBS. A dye, *N*-phenylnaphthylamine (NPN), was added to 10 mL of the bacterial suspension to obtain a 10 μM concentration of the dye. Saturation of fluorescence in the bacterial suspension was achieved using excitation at 350 nm and emission at 420 nm. Following saturation, the cells were subjected to different treatments including rifampicin, **TAC6**, and combination treatments for a 15 min duration. The bacterial cells were then plated on a 96-well microtiter plate, and the fluorescence kinetics was set up for 30 min in a Spectramax M5 multimode

microplate reader (Molecular Devices, Sunnyvale, CA, USA). Similarly, the outer membrane permeabilization activity for all polymers was tested.

Inner membrane potential assay. Log phase bacterial cells were centrifuged at 5000 rpm for 10 min. The collected cells were resuspended in 1× PBS, and stained with 3,3′-diethylthiadicarbocyanine iodide ($DiSC_2(5)$) (100 μM). Cells were incubated at 37 °C to get a saturation in fluorescence emission at 670 nm with an excitation of 637 nm. To stabilize the fluorescence in the suspended cells, KCl (100 mM) was also added. These cells were then treated with different treatments and incubated for 15 min. The cells were transferred to a 96-well plate, and the fluorescence kinetics was set up in a Spectramax M5 multimode microplate reader (Molecular Devices, Sunnyvale, CA, USA) for 30 min.

Propidium iodide uptake assay. Bacterial cells were grown to log phase, then harvested at 5000 rpm for 10 min. Cells were resuspended in 1× PBS to 10^7 cells per mL, and administered treatments with individual and combination groups for an hour. Next, cells were stained with PI (10 μg mL^{-1}) and incubated for 10 min. Cells were then washed twice with 1× PBS, and subsequently resuspended in 100 μL of 1× PBS. Cells were analysed using flow cytometry under propidium iodide channel with a BD FACS Verse flow cytometer (BD Biosciences, San Jose, CA).

Reactive oxygen species generation assay. Bacterial cells growing in log phase were pelleted at 5000 rpm for 5 min. Approximately 10^8 CFU per mL of bacteria were treated with **TAC6**, rifampicin, and a combination of **TAC6** and rifampicin for 1 h at 37 °C. Cells were centrifuged at a high speed of about 12 000 rpm for 2 min. The supernatant was transferred to fresh tubes, and treated with 10 μM of DCFH-DA (dichlorofluorescin diacetate) for 1 h at 37 °C. ROS production was analyzed by measuring the fluorescence with an excitation/emission wavelength of 485 nm/535 nm using a Spectramax M5 multimode microplate reader (Molecular Devices, Sunnyvale, CA, USA).

Biofilm degradation studies. Bacterial cells were cultured in LB media up to log phase at 37 °C, and the bacterial suspension was diluted to get 5×10^6 CFU per mL in TSB with 1% glucose. The bacterial suspension was added to a sterile six-well plate having sterile coverslips (18 × 18 mm). The plates were incubated at 37 °C for 14 h, and the media was changed for fresh LB media after 14 h. The condensed biofilms were treated for different time points (0, 2, 4, 8, and 12 h). At each time point, the biofilms were washed in 1× PBS and treated with 1× trypsin (100 μL) for 2–3 min. The biofilms were resuspended in LB media, and serially diluted followed by plating on LB agar plates. The plates were incubated at 37 °C for 16–18 h, and evaluation of viable bacterial cells was performed by assessment of colony forming units (CFUs). Another set of the biofilms was treated for 12 h, and stained with 1 μL of a 1 : 1 mixture of SYTO-9 and PI from the LIVE/DEAD Baclight bacterial viability and counting kit. The biofilm images were then obtained under a confocal microscope, Leica TCS SP8, Germany.

Animal studies.[50] Male BALB/c mice (average weight ~20 g, age ~6–8 weeks) were given ketamine and xylazine (100 μL per mice) by intraperitoneal injection to induce anesthesia, and the dorsal fur was shaved and cleaned using Veet hair removal cream. The naked skin of mice was sterilized with povidone iodine solution. A pair of scissors was used to create an open wound with diameter of ~1 cm. We infected the wound with 20 μL of *P. aeruginosa* bacterial suspension (~10^6 cells). After 18 h of infection, the mice were divided into four groups. The first group of mice was treated with saline, and the second group was treated with rifampicin (5 mg kg^{-1}, three times a day). The third group of mice was treated with **TAC6** (10 mg kg^{-1}, three times a day), and the fourth group was treated with a combination of **TAC6** (5 mg kg^{-1}) and rifampicin (5 mg kg^{-1}) three times daily, and the treatment was continued for the next 3 days. On the fourth day, we sacrificed mice from each group and quantified the bacterial burden *via* CFU analysis.

Ethical statement

Animal experimental protocols were reviewed and approved by the Institutional Animal Ethics Committee of the Regional Centre for Biotechnology (RCB/IAEC/2019/054). The experiments were carried out as per the guidelines issued by the Committee for the Purpose of Control and Supervision of Experiments on Animals (CPCSEA), Govt of India.

Author contributions

NC and BA performed all *in vitro* and animal experiments. VS supervised the bacterial experiments. PSY and AS provided the compounds. AB conceived the idea and supervised the project.

Conflicts of interest

Authors declare no competing financial interest.

Acknowledgements

We thank RCB for intramural funding, and the Department of Biotechnology (DBT) Govt of India for supporting the work in AB's laboratory. The students thank the funding agencies CSIR, UGC, and RCB for the research fellowship. The animal work in the small animal facility of the Regional Centre for Biotechnology is supported by BT/PR5480/INF/22/158/2012 (DBT). We acknowledge the support of the DBT e-Library Consortium (DeLCON) for providing access to e-resources. Fig. 8 and the TOC figure were prepared using BioRender.com.

Notes and references

1 J. P. Horcajada, M. Montero, A. Oliver, L. Sorlí, S. Luque, S. Gómez-Zorrilla, N. Benito and S. Grau, Epidemiology and treatment of multidrug-resistant and extensively drug-

resistant *Pseudomonas aeruginosa* infections, *Clin. Microbiol. Rev.*, 2019, **32**, 31–19.
2 S. L. Gellatly and R. E. Hancock, *Pseudomonas aeruginosa*: new insights into pathogenesis and host defenses, *Pathog. Dis.*, 2013, **67**, 59–173.
3 R. Serra, R. Grande, L. Butrico, A. Rossi, U. F. Settimio, B. Caroleo, B. Amato, L. Gallelli and S. de Franciscis, Chronic wound infections: The role of *Pseudomonas aeruginosa*, and *Staphylococcus aureus*, *Expert Rev. Anti-Infect. Ther.*, 2015, **13**, 605–613.
4 K. H. Turner, J. Everett, U. Trivedi, K. P. Rumbaugh and M. Whiteley, Requirements for *Pseudomonas aeruginosa* acute burn and chronic surgical wound infection, *PLoS Genet.*, 2014, **10**, e1004518.
5 N. M. Maurice, B. Bedi and R. T. Sadikot, *Pseudomonas aeruginosa* biofilms: Host response and clinical implications in lung infections, *Am. J. Respir. Cell Mol. Biol.*, 2018, **58**, 428–439.
6 P. K. Taylor, A. T. Yeung and R. E. Hancock, Antibiotic resistance in *Pseudomonas aeruginosa* biofilms: Towards the development of novel anti-biofilm therapies, *J. Biotechnol.*, 2014, **191**, 121–130.
7 S. Wagner, R. Sommer, S. Hinsberger, C. Lu, R. W. Hartmann, M. Empting and A. Titz, Novel strategies for the treatment of *Pseudomonas aeruginosa* infections, *J. Med. Chem.*, 2016, **59**, 5929–5969.
8 M. Bassetti, A. Vena, A. Croxatto, E. Righi and B. Guery, How to manage *Pseudomonas aeruginosa* infections, *Drugs Context.*, 2018, **7**, 212527.
9 Z. Breijyeh, B. Jubeh and R. Karaman, Resistance of Gram-negative bacteria to current antibacterial agents and approaches to resolve it, *Molecules*, 2020, **25**, 1340.
10 H. Nikaido, Molecular basis of bacterial outer membrane permeability revisited, *Microbiol. Mol. Biol. Rev.*, 2003, **67**, 593–656.
11 B. W. Simpson and M. S. Trent, Pushing the envelope: LPS modifications and their consequences, *Nat. Rev. Microbiol.*, 2019, **17**, 403–416.
12 B. D. Needham and M. S. Trent, Fortifying the barrier: The impact of lipid A remodelling on bacterial pathogenesis, *Nat. Rev. Microbiol.*, 2013, **11**, 467–481.
13 M. M. Konai and J. Haldar, Lysine-based small molecule sensitizes rifampicin and tetracycline against multidrug-resistant *Acinetobacter baumannii* and *Pseudomonas aeruginosa*, *ACS Infect. Dis.*, 2020, **6**, 91–99.
14 V. B. Hubble, K. R. Bartholomew, A. W. Weig, S. M. Brackett, S. L. Barlock, A. E. Mattingly, A. M. Nemeth, R. J. Melander and C. Melander, Augmenting the activity of macrolide adjuvants against *Acinetobacter baumannii*, *ACS Med. Chem. Lett.*, 2020, **11**, 1723–1731.
15 M. Tyers and G. D. Wright, Drug combinations: A strategy to extend the life of antibiotics in the 21st century, *Nat. Rev. Microbiol.*, 2019, **17**, 141–155.
16 R. J. Worthington and C. Melander, Combination approaches to combat multidrug-resistant bacteria, *Trends Biotechnol.*, 2013, **31**, 177–184.
17 E. E. Gill, O. L. Franco and R. E. Hancock, Antibiotic adjuvants: diverse strategies for controlling drug–resistant pathogens, *Chem. Biol. Drug Des.*, 2015, **85**, 56–78.
18 H. Douafer, V. Andrieu, O. Phanstiel IV and J. M. Brunel, Antibiotic adjuvants: Make antibiotics great again, *J. Med. Chem.*, 2019, **62**, 8665–8681.
19 G. D. Wright, Antibiotic adjuvants: Rescuing antibiotics from resistance, *Trends Microbiol.*, 2016, **24**, 862–871.
20 Y. Liu, R. Li, X. Xiao and Z. Wang, Antibiotic adjuvants: An alternative approach to overcome multi-drug resistant Gram-negative bacteria, *Crit. Rev. Microbiol.*, 2019, **45**, 301–314.
21 M. Song, Y. Liu, X. Huang, S. Ding, Y. Wang, J. Shen and K. Zhu, A broad-spectrum antibiotic adjuvant reverses multidrug-resistant Gram-negative pathogens, *Nat. Microbiol.*, 2020, **5**, 1040–1050.
22 J. M. Stokes, C. R. MacNair, B. Ilyas, S. French, J. P. Côté, C. Bouwman, M. A. Farha, A. O. Sieron, C. Whitfield, B. K. Coombes and E. D. Brown, Pentamidine sensitizes Gram-negative pathogens to antibiotics and overcomes acquired colistin resistance, *Nat. Microbiol.*, 2017, **2**, 17028.
23 R. E. Hancock and G. Diamond, The role of cationic antimicrobial peptides in innate host defences, *Trends Microbiol.*, 2000, **8**, 402–410.
24 K. A. Brogden, Antimicrobial peptides: Pore formers or metabolic inhibitors in bacteria?, *Nat. Rev. Microbiol.*, 2005, **3**, 238–250.
25 F. Nederberg, Y. Zhang, J. P. Tan, K. Xu, H. Wang, C. Yang, S. Gao, X. D. Guo, K. Fukushima, L. Li and J. L. Hedrick, Biodegradable nanostructures with selective lysis of microbial membranes, *Nat. Chem.*, 2011, **3**, 409–414.
26 C. Tantisuwanno, F. Dang, K. Bender, J. D. Spencer, M. E. Jennings, H. A. Barton and A. Joy, Synergism between rifampicin and cationic polyurethanes overcomes intrinsic resistance of *Escherichia coli*, *Biomacromolecules*, 2021, **22**, 2910–2920.
27 Z. Si, H. W. Lim, M. Y. Tay, Y. Du, L. Ruan, H. Qiu, R. Zamudio-Vazquez, S. Reghu, Y. Chen, W. S. Tiong and K. Marimuthu, A glycosylated cationic block poly (β-peptide) reverses intrinsic antibiotic resistance in all ESKAPE Gram-negative bacteria, *Angew. Chem., Int. Ed.*, 2020, **59**, 6819–6826.
28 S. Barman, S. Mukherjee, S. Ghosh and J. Haldar, Amino-acid-conjugated polymer–rifampicin combination: Effective at tackling drug-resistant Gram-negative clinical isolates, *ACS Appl. Bio Mater.*, 2019, **2**, 5404–5414.
29 L. Zhai, Z. Zhang, Y. Zhao and Y. Tang, Efficient antibacterial performance and effect of structure on property based on cationic conjugated polymers, *Macromolecules*, 2018, **51**, 7239–7247.
30 S. Zhao, W. Huang, C. Wang, Y. Wang, Y. Zhang, Z. Ye, J. Zhang, L. Deng and A. Dong, Screening and matching amphiphilic cationic polymers for efficient antibiosis, *Biomacromolecules*, 2020, **21**, 5269–5281.
31 H. Adelnia, H. D. Tran, P. J. Little, I. Blakey and H. T. Ta, Poly (aspartic acid) in biomedical applications: From

polymerization, modification, properties, degradation, and biocompatibility to applications, *ACS Biomater. Sci. Eng.*, 2021, **7**, 2083–2105.

32 P. S. Yavvari, S. Gupta, D. Arora, V. K. Nandicoori, A. Srivastava and A. Bajaj, Clathrin-independent killing of intracellular mycobacteria and biofilm disruptions using synthetic antimicrobial polymers, *Biomacromolecules*, 2017, **18**, 2024–2033.

33 B. D. Quan, M. Wojtas and E. D. Sone, Polyaminoacids in biomimetic collagen mineralization: Roles of isomerization and disorder in polyaspartic and polyglutamic acids, *Biomacromolecules*, 2021, **22**, 2996–3004.

34 S. Zakharchenko, E. Sperling and L. Ionov, Fully biodegradable self-rolled polymer tubes: A candidate for tissue engineering scaffolds, *Biomacromolecules*, 2011, **12**, 2211–2215.

35 P. S. Yavvari, A. K. Awasthi, A. Sharma, A. Bajaj and A. Srivastava, Emerging biomedical applications of polyaspartic acid-derived biodegradable polyelectrolytes and polyelectrolyte complexes, *J. Mater. Chem. B*, 2019, **7**, 2102–2122.

36 K. Richardson, O. T. Bennion, S. Tan, A. N. Hoang, M. Cokol and B. B. Aldridge, Temporal and intrinsic factors of rifampicin tolerance in mycobacteria, *Proc. Natl. Acad. Sci. U. S. A.*, 2016, **113**, 8302–8307.

37 M. Toosky and B. Javid, Novel diagnostics and therapeutics for drug-resistant tuberculosis, *Br. Med. Bull.*, 2014, **110**, 129–140.

38 G. L. Mandell, The antimicrobial activity of rifampin: emphasis on the relation to phagocytes, *Rev. Infect. Dis.*, 1983, **5**, S463–S467.

39 I. M. Helander and T. Mattila-Sandholm, Fluorometric assessment of Gram-negative bacterial permeabilization, *J. Appl. Microbiol.*, 2000, **88**, 213–219.

40 J. D. Te Winkel, D. A. Gray, K. H. Seistrup, L. W. Hamoen and H. Strahl, Analysis of antimicrobial-triggered membrane depolarization using voltage sensitive dyes, *Front. Cell Dev. Biol.*, 2016, 29.

41 E. Eruslanov and S. Kusmartsev, Identification of ROS using oxidized DCFDA and flow-cytometry, in *Advanced protocols in oxidative stress II*, 2010, vol. 594, pp. 57–72.

42 L. A. Clifton, M. W. Skoda, A. P. Le Brun, F. Ciesielski, I. Kuzmenko, S. A. Holt and J. H. Lakey, Effect of divalent cation removal on the structure of Gram-negative bacterial outer membrane models, *Langmuir*, 2015, **31**, 404–412.

43 D. Sharma, L. Misba and A. U. Khan, Antibiotics versus biofilm: an emerging battleground in microbial communities, *Antimicrob. Resist. Infect. Control*, 2019, **8**, 1–10.

44 S. Gupta, J. Thakur, S. Pal, R. Gupta, D. Mishra, S. Kumar, K. Yadav, A. Saini, P. S. Yavvari, M. Vedantham and A. Singh, Cholic acid–peptide conjugates as potent antimicrobials against interkingdom polymicrobial biofilms, *Antimicrob. Agents Chemother.*, 2019, **63**, e00520–e00519.

45 B. A. Lipsky and C. Hoey, Topical antimicrobial therapy for treating chronic wounds, *Clin. Infect. Dis.*, 2009, **49**, 1541–1549.

46 R. S. Howell-Jones, M. J. Wilson, K. E. Hill, A. J. Howard, P. E. Price and D. W. Thomas, A review of the microbiology, antibiotic usage and resistance in chronic skin wounds, *J. Antimicrob. Chemother.*, 2005, **55**, 143–149.

47 R. J. Worthington, C. A. Bunders, C. S. Reed and C. Melander, Small molecular suppression of carbapenem resistance in NDM-1 producing *Klebsiella pneumoniae*, *ACS Med. Chem. Lett.*, 2012, **3**, 357–361.

48 J. H. Jorgensen, J. F. Hindler, L. B. Reller and M. P. Weinstein, New consensus guidelines from the Clinical and Laboratory Standards Institute for antimicrobial susceptibility testing of infrequently isolated or fastidious bacteria, *Clin. Infect. Dis.*, 2007, **44**, 280–286.

49 G. Orhan, A. Bayram, Y. Zer and I. Balci, Synergy tests by E test and checkerboard methods of antimicrobial combinations against Brucella melitensis, *J. Clin. Microbiol.*, 2005, **43**, 140–143.

50 K. Yadav, S. Kumar, D. Mishra, M. Asad, M. Mitra, P. S. Yavvari, S. Gupta, M. Vedantham, P. Ranga, V. Komalla, S. Pal, P. Sharma, A. Kapil, A. Singh, N. Singh, A. Srivastava, L. Thukral and A. Bajaj, Deciphering the role of intramolecular networking in cholic acid–peptide conjugates (CAPS) at lipopolysaccharide surface in combating Gram-negative bacterial infections, *J. Med. Chem.*, 2019, **62**, 1875–1886.